

Changes in Molecular Dynamics during the Bulk Polymerization of an Epoxide/Diamine Mixture Containing Inert Diluents as Studied Using Dielectric Relaxation Spectroscopy

Graham Williams,* Ian Karl Smith, and George A. Aldridge

Department of Chemistry, University of Wales Swansea, Singleton Park, Swansea SA2 8PP, U.K.

Paul A. Holmes and Su Varma

Pilkington Technology Centre, Hall Lane, Lathom, Ormskirk, Lancashire L40 5UF, U.K.

Received February 23, 2001; Revised Manuscript Received June 26, 2001

ABSTRACT: The evolution of the dielectric α relaxation and ionic conductivity with time t_r during polymerization at 60 °C of mixtures of the diepoxide DGEBA, the diamine PACM, and the diluent Decalin (DEC) or di-*n*-butyl phthalate (DBP) has been studied using real-time dielectric relaxation spectroscopy (DRS). Data are presented as permittivity $\epsilon(\omega, t_r)$ and impedance $Z(\omega, t_r)$. For $c_{\text{dil}} \leq 20\%$ (w/w), the main effect of diluent was to displace the α process to higher frequencies and, therefore, to increase the time required for glass formation over that for the unplasticized system. At higher values of c_{dil} , the behavior of $\epsilon(\omega, t_r)$ for DGEBA/PACM/DBP systems was more complex as the properties became stationary at long times, showing that an elastomer rather than a glass was formed. The results are discussed in relation to the “floor temperature” T_F for reaction introduced previously. The same data are presented as $Z(\omega, t_r)$, which emphasizes changes in the ac ionic conductivity with time. As for the ϵ data, qualitative differences are observed for the behavior of $Z(\omega, t_r)$ at low and high values of c_{dil} . It is demonstrated that changes in molecular mobility with time for all systems can be judged by the behavior of $\epsilon(\omega, t_r)$ but not by that of $Z(\omega, t_r)$ for these systems. The Fuoss–Kirkwood and KWW relaxation functions are used to express the half-width $\Delta \log t$ of the plot of ϵ'' vs $\log t_r$ at fixed measuring frequencies for a reactive system. The changes in $\Delta \log t$ with f and composition for the systems that became glasses are explained in terms of changes with time of (i) the width of the relaxation function and (ii) $[\Delta \log \langle \tau_\alpha \rangle / \Delta \log t_r]$, where $\langle \tau_\alpha \rangle$ is the average relaxation time. The behavior of $\langle \tau_\alpha(t_r) \rangle$ with time during reaction is considered in terms of the Angell fragility index m of the process. It is shown that (i) m increases during reaction for a given mixture and (ii) m , at fixed frequency, decreases as c_{dil} is increased.

Introduction

To modify the physical properties of epoxide-based thermosetting polymers for their applications as adhesives, coatings, engineering materials, and electrical insulators, the products are often made by curing mixtures containing soluble elastomers, thermoplastics, plasticizers, or other additives. At room temperature, the product of reaction can be a glass, viscoelastic solid, elastomer, or glass/rubber composite, depending on the formulation of the original mixture, and thus, materials are provided that exhibit a range of mechanical and electrical properties. Different techniques can be used to monitor the physical and chemical changes that occur during bulk thermosetting reactions. These include dynamic mechanical thermal analysis (DMTA), differential scanning calorimetry (DSC), IR and Raman spectroscopies, and dielectric relaxation spectroscopy (DRS). The real-time DRS technique is of value because it covers a wide frequency range (typically from 1 to 10^5 Hz) and can monitor changes during reaction of (i) the reorientational dynamics of dipole groups, (ii) α conductivity arising from extrinsic or intrinsic ions, and (iii) interfacial (Maxwell–Wagner) polarization. DRS studies have been made for bulk thermosetting reactions by several groups: see, e.g., the publications, inter alia, of Senturia and Sheppard, Kranbuehl, Rolla, Johari and Tombari, Mijovic, Pethrick, Maistros, Deng and Martin, and Fournier and Williams and their co-workers listed in ref 1. Also, bulk photostetting reactions involving free-radical reactions of acrylate and methacrylate mono-

mers have been studied: see, e.g., the works of Rolla and of Fournier and Williams and their co-workers listed in ref 1. For homogeneous thermosetting reactions, the product at a reaction temperature T_R can be a glass, viscoelastic solid, or elastomer. Williams and co-workers^{1,2} have shown that there is a floor temperature T_F below which a glass is formed and above which an elastomer is formed. The relationship between T_F and $T_{g\infty}$ introduced by Gillham³ in relation to his TTT diagram for thermosetting systems is discussed in ref 2. If the product of the reaction is a glass, a decrease in molecular mobility during reaction leads to diffusion control of the reaction rate, and this can be monitored by DRS measurements.^{1,2,4} Thermosetting polymerizations can involve phase separation of an inert component (elastomer or thermoplastic) from the reaction mixture, and this produces inhomogeneous blends (polymer composites) that have diverse practical applications. Partridge and Maistros⁵ have reviewed real-time DRS studies for such systems where phase separation of an elastomer was monitored through the marked increase in the Maxwell–Wagner interfacial polarization process with time.

The physical properties of thermosetting polymers can also be modified by inclusion of low-molar-mass diluents that act as plasticizers, lowering the glass transition temperature (T_g) of the initial mixture and the product. We previously studied⁴ the reaction of stoichiometric DGEBA/PACM mixtures at different temperatures using (i) real-time DRS to monitor changes in molecular

mobility and (ii) isothermal DSC to monitor changes in the extent of reaction with time. Comparison of the DRS and DSC data allowed correlations to be made between changes in molecular mobility and extent of reaction,⁴ showing that at the temperatures studied the systems became glasses at long times through the onset of diffusion control through a lack of molecular mobility, as had been previously demonstrated for related epoxide/amine systems (see, e.g., ref 1 for a listing of those studies). In the present work, real-time DRS is used to monitor changes in the dipole relaxations and the ionic conduction of reactive epoxide/amine systems containing Decalin (DEC) or di-*n*-butyl phthalate (DBP) as diluents. DEC has essentially zero dipole moment, so relaxation in the DGEBA/PACM/DEC system (see below) arises from the motions of the epoxide and amine dipoles and their reaction products. DBP has an appreciable dipole moment and so makes a contribution to the overall dipole relaxation. The present studies (i) provide a means of determining how the molecular dynamics of a reactive system varies with diluent concentration where the product can be an elastomer or a glass and (ii) make connections to our earlier work concerning the floor temperature.^{1,2} We have not conducted parallel studies of the extent of cure as reaction occurs, which would have extended the experimental work considerably. Recently, in a wide-ranging and important study, Andjelic and Mijovic⁶ made comparative studies, using real-time DRS (for molecular dynamics) and NIR Fourier transform spectroscopy (for chemical conversion), of reactions of different compositions of mixtures containing stoichiometric amounts of DGEBA and 4,4'-methylenedianiline (MDA) together with the nonpolar diluent *o*-terphenyl (OT). Our present results will be compared below with those of Andjelic and Mijovic.

Experimental Section

The diepoxide was the diglycidyl ether of bisphenol A (DGEBA), provided by Shell Chemicals as Epicoate 828. The diamine was the alicyclic diamine 4,4'-diaminodicyclohexylmethane (PACM), provided by Anchor Chemicals. Decalin (DEC) and di-*n*-butyl phthalate (DBP) were obtained from Aldrich Chemicals. Each sample was prepared for DRS measurements by adding a given amount of diluent to a stoichiometric mixture prepared in the ratio 2 mol of DGEBA to 1 mol of PACM. DEC was added as 10 and 20% (w/w), and DBP as 10, 20, 30, and 40% (w/w). The samples were made by weighing out the components into a sample tube and then stirring vigorously for 10 min at room temperature to achieve a homogeneous liquid. All initial mixtures and products were optically transparent, so there was no evidence of phase separation of the diluent during reaction. An initial mixture was poured into a parallel-plate dielectric cell that was placed in a Novocontrol BDS 1200 sample holder. DRS measurements were made using a Novocontrol dielectric spectrometer that incorporated a Solartron 1260 impedance analyzer and a Chelsea dielectric interface as we have previously described.^{1,2,7} Measurements were initiated from the time the sample reached the reaction temperature. The heating process took approximately 5 min in each experiment. All studies reported here were made with $T_R = 60^\circ\text{C}$. DRS measurements were made in the range $0 \leq \log(f/\text{Hz}) \leq 5$ in steps of 0.2 (in units of $\log f$), giving 26 frequencies in each sweep, which took approximately 3 min. To have an almost continuous measurement of the DRS properties, the sweeps were programmed to take place at 200-s intervals. The time t_i of each measurement at each frequency $f (= \omega/2\pi)$ was recorded, giving DRS data as the real permittivity $\epsilon'(\omega, t_i)$ and the dielectric loss factor $\epsilon''(\omega, t_i)$. Graphical presentations of the data generated by the Novocontrol spectrometer were made using Axum programs.

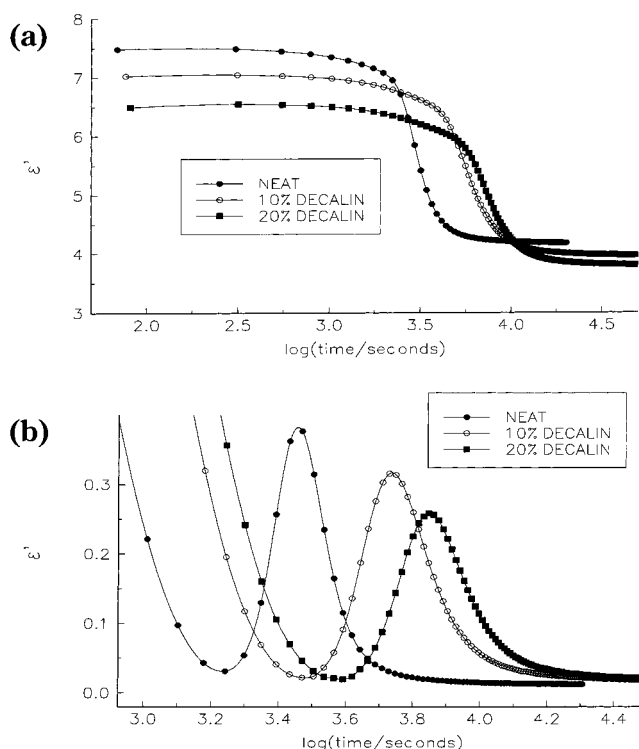


Figure 1. (a) ϵ' and (b) ϵ'' vs $\log(t/s)$ for DGEBA/PACM/DEC systems measured at $f = 1$ kHz during reaction at 60°C .

One objective of the study was to compare the DRS behavior of different DGEBA/PACM/DEC and DGEBA/PACM/DBP mixtures. DGEBA and PACM, in common with other organic materials containing strongly reactive groups, age chemically during storage in the presence of moisture and air. Therefore, all DRS measurements of the DGEBA/PACM/DBP systems were made in the same time period. Similarly, those for the DGEBA/PACM/DEC systems were made in the same time period, but one different from that for the DBP-containing systems.

Results and Discussion

DGEBA/PACM/DEC Systems. As an example of the DRS data, Figure 1 shows plots of ϵ' and ϵ'' vs $\log(\text{time}/s)$ for $f = 1$ kHz and $T_R = 60^\circ\text{C}$ for mixtures containing 0, 10, and 20% Decalin. In accordance with previous studies,^{1-3,7} the dispersion of ϵ' and the peak in ϵ'' with time are due to the α -relaxation process that arises from the micro-Brownian motions of all dipoles in the system at time t_i . The initial losses are due to the conduction of ions in the reacting mixture and fall rapidly with time. The maximum loss ϵ''_{max} decreases with increasing c_{dec} , reflecting the reduction of the dipole concentration in the mixture. As c_{dec} increases, the peaks move to longer times, showing that the time required for a reacting mixture to form a glass increases accordingly. Data as in Figure 1 were obtained at all 26 frequencies for each system. They were combined to yield (i) 3D plots of ϵ' and ϵ'' vs $[\log(f/\text{Hz}), \log(t_i)]$ (dielectric landscapes) and (ii) 2D plots of these quantities vs $\log(f/\text{Hz})$ at fixed values of t_i . As an example, Figure 2 shows 3D plots for the 20% Decalin blend at 60°C . The dipole loss peak (α relaxation) is well-separated from the conductivity-related losses at short times and low frequencies. The α process, although sharp in the isofrequency plots (Figure 1b), is extremely broad in plots of ϵ'' vs $\log(f/\text{Hz})$, with width at half-height $\Delta \log f > 3.5$. Consider now the information contained in plots of ϵ'' vs $\log(t_i/s)$ at constant frequency and ϵ'' vs $\log(f/\text{Hz})$ at constant

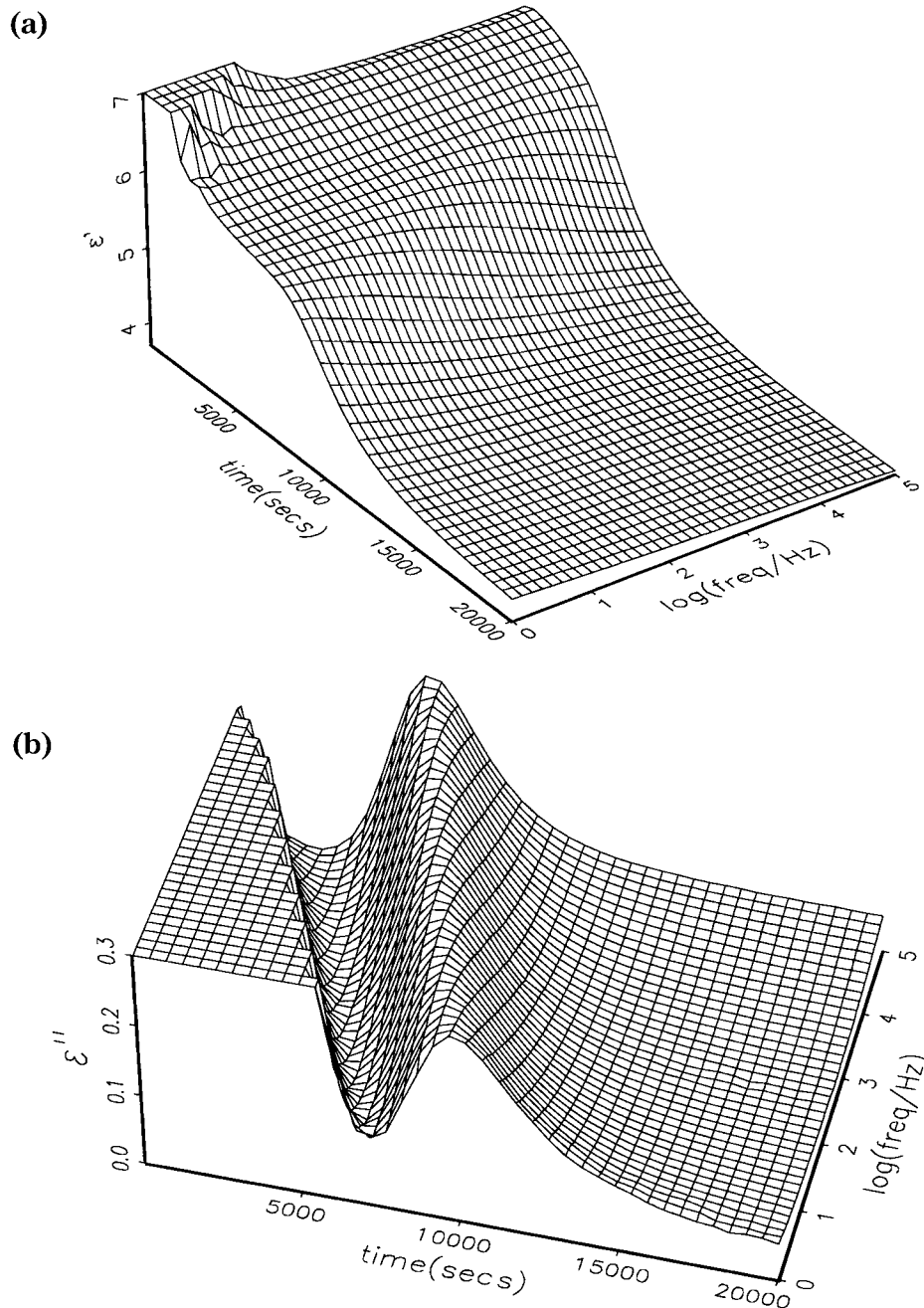


Figure 2. (a) ϵ' and (b) ϵ'' vs $\log(f/\text{Hz})$ and $\log(t_r/\text{s})$ for the 20% Decalin system.

time. The loss curves in the frequency domain can be fitted using different empirical functions. Consider first the Fuoss–Kirkwood equation (see ref 8, p 117).

$$\epsilon'' = 2\epsilon''_{\max} \frac{(\omega\tau)^n}{1 + (\omega\tau)^{2n}} \quad (1)$$

where τ is the relaxation time [$\tau = (2\pi f_{\max})^{-1}$], where f_{\max} is the frequency of maximum loss. n is the spread parameter, $0 \leq n \leq 1$. Thus, f and τ are complementary variables. In plots of ϵ'' vs $\log(f/\text{Hz})$, τ is constant, while f varies. In plots of ϵ'' vs $\log(t_r/\text{s})$ (e.g., Figure 1b), f is constant, while τ varies as $\tau(t_r)$. We have shown⁹ that the loci of the points [$\log(f_{\max})$, $\log(t_r)$] and [$\log(f)$, $\log(t_r \max)$] lie on a common line for the neat DGEBA/PACM system. f_{\max} and $t_r \max$ refer to the condition of maximum loss in each plot. Thus, the changes in $\tau(t_r)$ with reaction time t_r can be determined from either plot for this case.

Figure 3 shows the plots of $\log(f/\text{Hz})$ vs $\log(t_r \max/\text{s})$ for the 0, 10, and 20% Decalin systems as obtained from Figure 1b and our data at the other frequencies. These plots monitor the movement of the α process to low frequencies as the reaction proceeds. The plots curve downward with f reaching 1 Hz, showing that these reaction mixtures become glasses at long times. This means that $T_R = 60^\circ\text{C}$ is below the floor temperature T_F for these three mixtures.^{1,2}

In Figure 1a, the limiting value of ϵ' at long times, $\epsilon_{\infty\alpha}$ say, for the 0% Decalin (i.e., neat) system is ~ 4.2 which is far greater than the high-frequency value $\epsilon_{\infty} \approx 2\text{--}2.5$ expected for an immobile organic glass. Thus, dipole motions are extensive in the glassy product, and a β process⁸ occurs at frequencies higher than our range. $\epsilon_{\infty\alpha}$ decreases with increasing c_{dec} , which is partly due to the dilution effect of the nonpolar Decalin. Figure 4 gives plots of ϵ' and ϵ'' vs $\log(f/\text{Hz})$ recorded at the

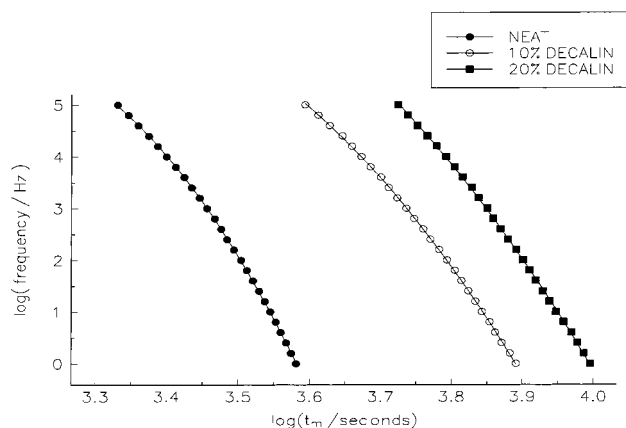


Figure 3. $\log(f/\text{Hz})$ vs $\log(t_{\max}/s)$ for the α process in 0, 10, and 20% Decalin systems.

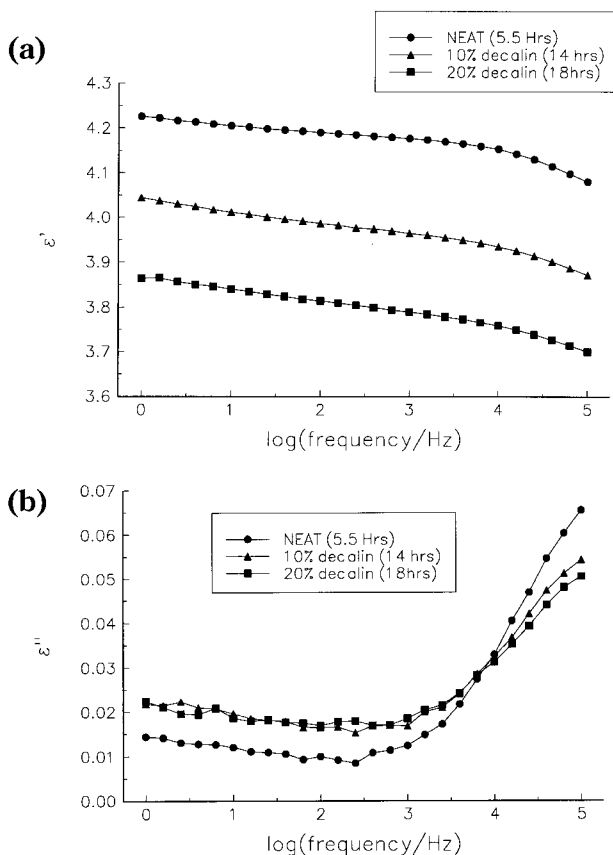


Figure 4. (a) ϵ' and (b) ϵ'' vs $\log(f/\text{Hz})$ for the 0, 10, and 20% Decalin systems at 5.5, 14 and 18 h during reaction at 60 °C.

longest reaction times for each system at 60 °C, showing the fall in ϵ' and the rise in ϵ'' with increasing frequency due to the β process. The fall in $\epsilon_{\infty\alpha}$ with c_{dec} is greater than expected from the dilution effect and suggests that the relaxation strength $\Delta\epsilon_{\beta}$ actually decreases with increasing diluent concentration, i.e., the Decalin molecules block the local motions, transferring the relaxation strength to the α process.

Thus, the behavior of the α relaxation during reaction has been determined for systems that comprise a stoichiometric mixture of epoxide and diamine, together with the nonpolar diluent in the range 0–20% DEC. The α process, represented as $\epsilon'(\omega, t_r)$ and $\epsilon''(\omega, t_r)$, moves to longer times as the reaction proceeds. The effective time to form a glass increases with increasing diluent concentration. This can be rationalized as follows. The T_g

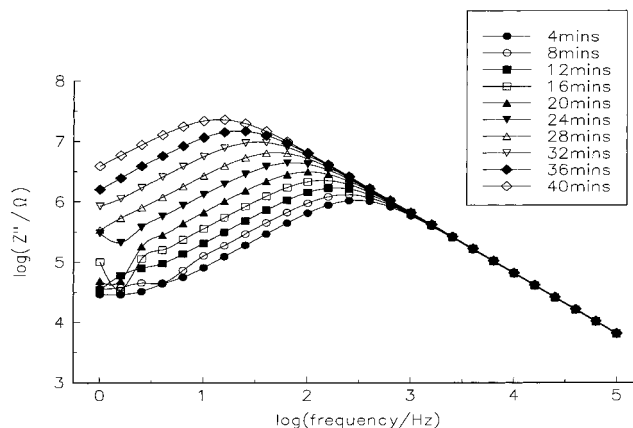


Figure 5. $\log(-Z''(f))$ vs $\log(f/\text{Hz})$ for the 20% Decalin system at different times.

of the neat initial mixture, M_0 say, is $T_g(0)_0$. As the reaction proceeds, $T_g(t_r)$ increases until T_R is reached,² when diffusion control effectively suppresses further reaction through reduced molecular mobility.^{1,2} The T_g for an initial mixture containing Decalin, M_D say, is $T_g(0)_M$, where $T_g(0)_M < T_g(0)_0$. To form a glass, $T_g(t)$ must increase by $\Delta T_M = [T_R - T_g(0)_M]$ for M_D and $\Delta T_0 = [T_R - T_g(0)_0]$ for M_0 . Because $\Delta T_M > \Delta T_0$, the time taken to form a glass for M_D is greater than that for M_0 . A corollary is that, if the diluent were an “antiplasticizer” in the sense that $T_g(\text{diluent}) > T_g(0)_0$, then the time taken to form a glass starting with M_{diluent} would be less than that for M_0 , a result that might have practical applications for thermosetting systems that form a glass at T_R .

The same DRS data can be presented as complex impedance, $Z = Z' + iZ''$, as described by Mijovic and workers.^{10–12} As one example, Figure 5 shows $\log(-Z'')$ vs $\log(f/\text{Hz})$ determined at 4-min intervals in the range $4 \leq (t_r/\text{min}) \leq 40$ for the 20% Decalin system at 60 °C. The peaks are characteristic of a system in which Z'' is dominated by conductivity due to ionic species.^{2,10–13} Regarding the system as a parallel arrangement of a resistance R_p and a capacitance C_p , Z' is given by

$$Z' = -R_p \omega \tau_{RC} (1 + \omega^2 \tau_{RC}^2)^{-1} \quad (2)$$

where $\tau_{RC} = R_p C_p$. The plots in Figure 5 have slopes of +1 and –1 at low and high frequencies, respectively, and a peak at $\omega_{\max} \tau_{RC} = 2\pi f_{\max}(\omega) \tau_{RC} = 1$, where $f_{\max}(\omega)$ is the peak frequency. Also $Z'_{\max} = R_p/2$. The data fall on a common line at high frequencies because the values equal $(\omega C_p)^{-1}$, where C_p is approximately independent of t_r . At low frequencies, $|Z'|$ increases with time at fixed frequencies as $Z'(\text{low frequencies}) = -R_p \omega \tau_{RC}$ and R_p increases with time. Figure 6a and b shows plots of $\log(f_{\max}(\omega)/\text{Hz})$ and $\log(\sigma/(\text{S cm}^{-1}))$, respectively, vs time derived from Figure 5, where σ is the specific conductivity and is determined using $f_{\max}(\omega)$ values and the sample dimensions. As c_{dec} is increased the plots extend to longer times, that is, changes in ionic mobility, and hence σ , occur more slowly with time as a result of a retardation of the reaction rate. Figure 6a and the corresponding data for the 0 and 10% Decalin systems show that the peaks in Z'' move to 1 Hz at 1.7, 3.0, and 3.6 ks for the 0, 10, and 20% systems respectively, which are far shorter times than those required for $\log f$ from the ϵ'' data to reach 1 Hz (Figure 3). Molecular mobility, as judged by the ϵ'' data, is still rapid when $f_{\max}(\omega)$ falls

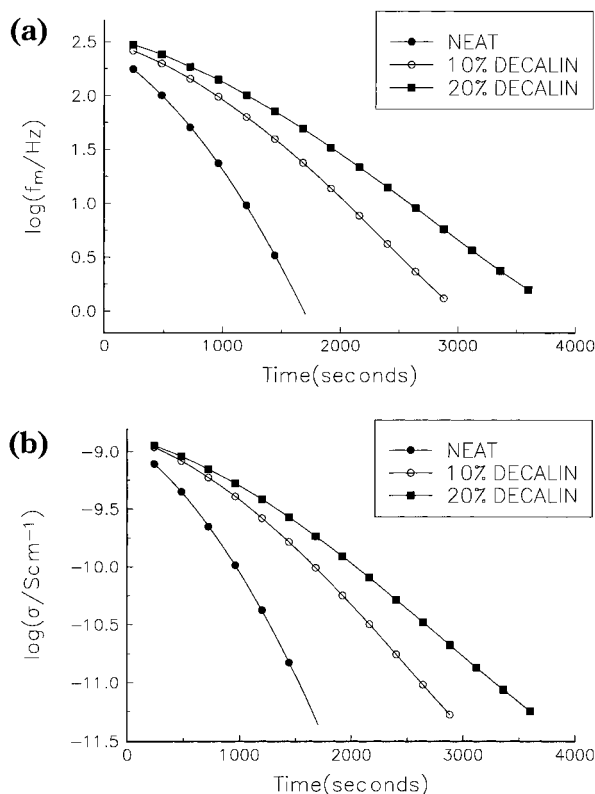


Figure 6. (a) $\log(f_{\max}(\omega)/\text{Hz})$ and (b) $\log(\sigma/S \text{ cm}^{-1})$ vs time/s for the 0, 10, and 20% Decalin systems.

to 1 Hz. This means that changes in *molecular mobility* during reactions that lead to glass formation at T_R should be monitored using the ϵ'' data and not the Z'' data for these systems.

It is of interest to compare the present data for the DGEBA/PACM/DC system with those of the important recent study by Andjelic and Mijovic⁶ for the DGEBA/MDA/OT system, where MDA and OT are 4,4'-methylenedianiline and *o*-terphenyl, respectively. In common with DEC, OT is essentially nondipolar, so it makes no contribution to the relaxation strength. Interestingly, the unreacted stoichiometric mixture of DGEBA and MDA has approximately the same T_g as OT (-19 and -23 °C, respectively, from DSC), so the loss peaks in the scans of ϵ'' vs temperature at 25 kHz occur at approximately the same temperature (0 °C in Figure 4 of ref 6). They studied the DRS behavior for unreacted mixtures and partially reacted mixtures of (DGEBA/MDA)/OT having initial compositions in the range 100/0 to 10/90 (w/w) and simultaneously monitored the extent of conversion $\alpha_c(t)$, using FT-NIR spectroscopy.⁶ They showed, inter alia, that the reaction rate decreased with increasing OT content, increasing the time required to form a glass. Our DRS data for the 0, 10, and 20% DEC systems (see Figure 3) are in accord with this result. They also obtained the plots of ϵ'' vs $(T/K)^{-1}$ for each of the *unreacted* mixtures (their Figure 6a and b) and for a series of partially reacted mixtures [see, e.g., their Figure 8 for an initial mixture of 50(DGEBA/MDA)/50 OT]. For the unreacted mixtures, the loci of the plots of $\log f_{\max}$ vs $(T/K)^{-1}$ were very similar. The plot for the 100/0 (neat) initial mixture was curved, whereas the plot for the 13/87 initial mixture was linear (Arrhenius behavior), which was interpreted as indicating that the diluent caused a weakening of the dipole–dipole interactions between molecules, leading to a decrease in the

“fragility”,¹⁴ or alternatively the “cooperativity”,¹⁵ of the dielectric α process. For the partially reacted mixtures, a complex pattern of behavior was observed.⁶ For an initial 50/50 or 33/67 mixture, the resultant partially cured materials in the range from 0 to ~35% conversion (their regime I) gave plots of $\log f_{\max}$ vs $(T/K)^{-1}$ that were approximately linear and nearly parallel (similar apparent activation energies, Q) as they moved to higher temperatures with time (T_g increasing with time). In the range from ~35 to 55% conversion (their regime II), Q decreases slightly, and then in the range 55 to 70% conversion (their regime III), Q increases markedly. They note that the change from regime II to regime III occurs in the vicinity of the gel point (~60% for the 50/50 formulation⁶). For the 100% (neat) initial mixture, the change in Q on going from regime II to regime III is less marked. They analyze this overall behavior in terms of changes in intermolecular dipole–dipole interactions and the formation of hydrogen-bonded complexes resulting from reaction, as modified by the presence of diluent. In our measurements, we obtained real-time DRS data during reaction for stoichiometric mixtures containing up to 20% DEC. Our plots of $\log f$ vs $\log t_r$ in Figure 3 reveal no significant changes in behavior that would indicate different regimes as each system forms a glass during isothermal polymerization at 60 °C.

Andjelic and Mijovic⁶ showed that, for the DGEBA/MDA/OT systems, the shape and half-widths ($\Delta_{1/2}$) of the α process varied in a complex way during polymerization. For an initial 50/50 formulation, the normalized loss peaks for 10, 20, 40, and 70% conversion were determined (their Figure 11) for each partially cured sample over a range of temperature, and the normalized distribution function $G(\tau)$ was determined. The loss curves for the 0 and 10% conversions resembled KWW behavior with $\Delta_{1/2} \approx 2$ ($\beta_{\text{KWW}} \approx 0.53$), and thus, $G(\tau)$ was asymmetric toward short times. In the range of 10–55% conversion, the loss curves broadened ($\Delta_{1/2}$ increased to ~3) and became more symmetrical giving $G(\tau)$ symmetrical with respect to $\log \tau/\tau_{\max}$. For 60 and 70% conversion, the loss curves were very broad ($\Delta_{1/2} \approx 6$), and $G(\tau)$ again became asymmetric toward short times. They concluded that, above 60% conversion, the behavior is related “to the effect on dipole dynamics by the chemophysical changes on the molecular level in the network at that stage of cure which are accompanied by the emergence of hydrogen-bonded complexes in neat and solvent-containing formulations alike”. The present studies (see, e.g., Figure 2) also extended to the ranges of cure in which first a gel and then a glass were formed. Our DRS data give clear evidence for glass formation at long times, because the α relaxation moves to ultralow frequencies (Figure 3), but provide no evidence for the onset of gel formation (see also ref 1 on this point). When the loss peaks for the three DGEBA/PACM/DEC systems appear in the frequency range from 1 to 10^5 Hz the curves are extremely broad, with $\Delta_{1/2} \geq 3$ at all times. For the reaction of the neat stoichiometric DGEBA/PACM mixture at 60 °C, the loss curves are asymmetrical in the KWW sense. $\Delta_{1/2}$ increases from 3.5 to 4 as time increases from 2200 to 3000 s. The same behavior applies to the DRS data for the 10 and 20% DGEBA/PACM/DEC systems. Thus, in the time range prior to that for glass formation, which is a region of high conversion for the neat system, $G(\tau)$ is extremely broad and asymmetrical in the KWW sense, and $\Delta_{1/2}$

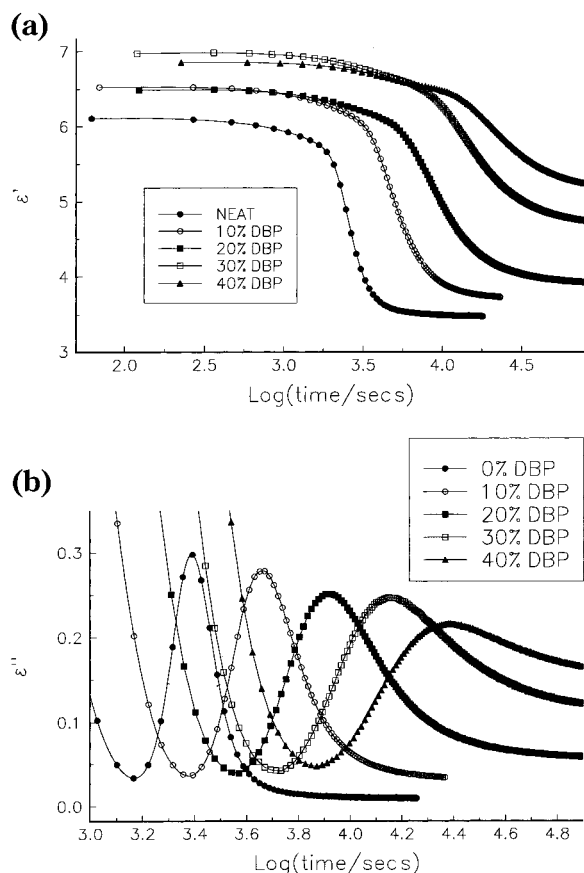


Figure 7. (a) ϵ' and (b) ϵ'' vs $\log(t/s)$ at 1 kHz for the 0, 10, 20, 30, and 40% DBP systems.

increases markedly with time. Such behavior is consistent with that observed by Andjelic and Mijovic⁶ at high conversions for their 50/50 formulation of (DGEBA/MDA)/OT (see ref 6, Figure 14d).

DGEBA/PACM/DBP Systems. In contrast to the DGEBA/PACM/DEC systems described above, DBP is strongly polar and therefore contributes to the dipolar relaxation in these systems. As examples of our data, Figures 7 and 8 show plots of ϵ' and ϵ'' vs $\log(t/s)$ for the 0, 10, 20, 30 and 40% DBP systems cured at 60 °C at measuring frequencies of 1 and 10 kHz, respectively. The ϵ' values plateau at short times (Figures 7a and 8a), even though there is considerably loss due to ionic conductivity at short times that might affect ϵ' . (Figures 7b and 8b). The α process moves to longer times as the percentage of DBP is increased, as expected because DBP, like Decalin, acts as a plasticizer. The static permittivities ϵ_0 increase from ~ 6.1 to ~ 7.0 (see Figures 7a and 8a) as DBP increases to 40%, reflecting the polarity of DBP in the mixture, whereas for the Decalin systems ϵ_0 decreases with increasing c_{DBP} (Figure 1a). Despite the increase in ϵ_0 , the loss peaks in Figures 7b and 8b decrease in height as c_{DBP} is increased, indicating a broadening of the distribution of relaxation times and/or a decrease in $[d \log \tau / d \log t_r]$, which will be considered below. For the 0, 10, and 20% DBP systems, loss peaks could be observed in plots of ϵ'' vs $\log t_r$ down to frequencies of 1 Hz, showing that a glass forms at long times in each case. Figure 9 shows plots of $\log(f/\text{Hz})$ vs $\log(t/s)$ for the 0, 10, and 20% DBP systems. As for DGEBA/PACM/DEC, the plots curve downward in each case and are displaced to longer times as c_{DBP} increases, showing the increase in the effective time to form a glass as the percentage of DBP is raised. Figure 10 shows

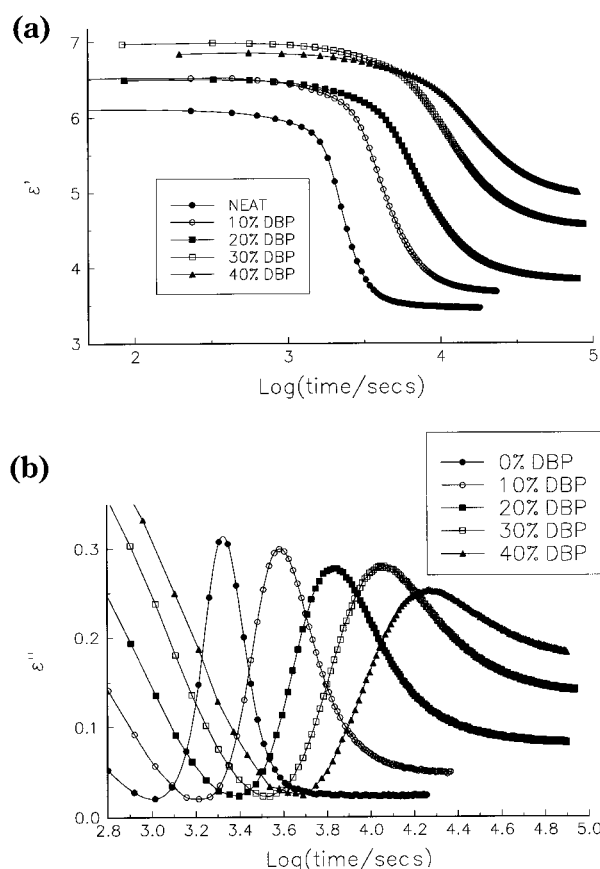


Figure 8. (a) ϵ' and (b) ϵ'' vs $\log(t/s)$ at 10 kHz for the 0, 10, 20, 30, and 40% DBP systems.

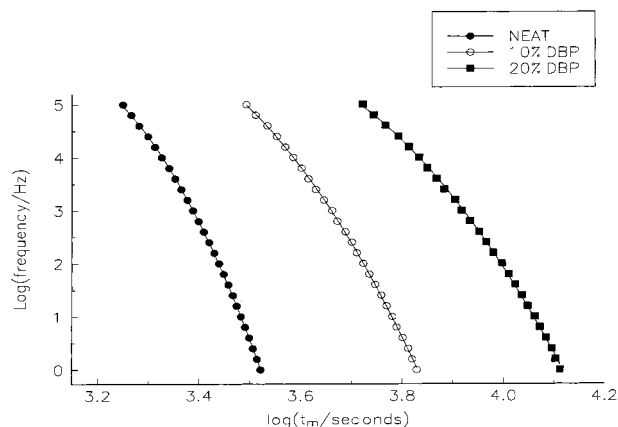


Figure 9. $\log(f/\text{Hz})$ vs $\log(t_{\text{max}}/s)$ for the 0, 10, and 20% DBP systems.

plots of ϵ'' vs $\log(f/\text{Hz})$ for the 20% DBP system. One broad dipole relaxation (the α process) moves through the f range as reaction proceeds. The β process is seen as a rising loss with increasing frequency at long times. In measurements that extend to 22 h (Figure 11), the α peak moves below 1 Hz, and its high-frequency tail is seen as the rising loss at low frequencies, while the peak of the β process remains above 100 kHz. Therefore, extensive local motions in the glass occur for this mixture, arising mainly from the DBP molecules. Consider again the ϵ data for the 30 and 40% DBP systems in Figures 7 and 8. In Figures 7a and 8a (30% and 40% DBP, respectively), the ϵ' values tend to plateau at long times with values greater than those expected for a glass, in contrast to the DGEBA/PACM/DEC systems (Figure 1). The loss values beyond the peak (Figures

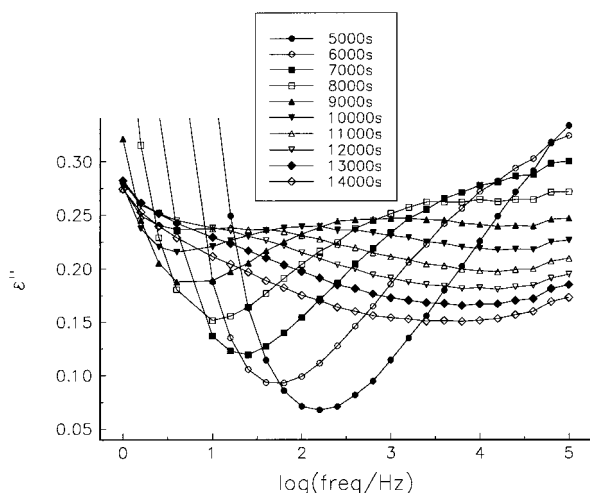


Figure 10. ϵ'' vs $\log(f/\text{Hz})$ for the 20% DBP system at different times during reaction.

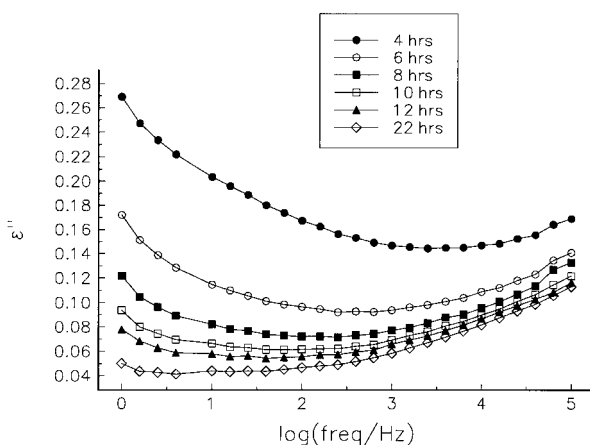


Figure 11. ϵ'' vs $\log(f/\text{Hz})$ for the 20% DBP system at very long times.

7b and 8b) tend to plateau as the percentage of DBP is increased. This behavior at long times is the same as that observed for an epoxide/boroxine system.^{1,2} In that case, for $T_R = 80^\circ\text{C}$, ϵ' fell at long times to plateau levels much larger than those of a glass and, whereas loss peaks were observed for $\log(f/\text{Hz}) = 5, 4, 3$ and 2 , ϵ'' rose to plateau levels for $\log(f/\text{Hz}) = 1$ and 0 with no evidence of a peak (see Figure 8 of ref 1). For that case, the reaction went to completion before diffusion control became operative. The system became an *elastomer* rather than a glass at long times, giving t -independent behavior for ϵ' and ϵ'' , i.e., the system at 80°C was above its floor temperature T_F .^{1,2} A similar situation applies to the DGEBA/PACM/DBP system for the higher values of c_{DBP} . The behavior as c_{DBP} is changed is also seen in the 3D plots of ϵ' and ϵ'' vs $[\log(f/\text{Hz}), \log(t/\text{s})]$ (Figures 12–15). For 10 and 20% DBP (Figures 12 and 13), the α relaxation moves to ultralow frequencies with time, showing that a glass is formed (for brevity, we do not show the equivalent data for 0% DBP). The behavior in Figures 14 and 15 for 30 and 40% DBP is more complex. ϵ''_{ions} values decrease rapidly as time and frequency increase. The α -loss peak is seen at higher frequencies, but its evolution with time is very different from that in Figures 12 and 13. There is no pronounced movement of the peak to low frequencies as seen for the 10 and 20% DBP systems (and DEC systems, e.g., Figure 2). For $\log(t/\text{s}) > 4.5$, the ϵ' and ϵ'' values plateau at levels far greater than those for a glass (cf. Figures 12 and

13). ϵ'' values increase with increasing frequency for $\log(t/\text{s}) > 4.5$, showing that there is a higher-frequency β process. This complex behavior is seen in the plots of ϵ'' vs $\log(f/\text{Hz})$ (Figures 16 and 17) for the 30 and 40% DBP systems. In Figure 16, at $t_r = 1$ h, the ϵ''_{ions} values decrease with increasing frequency to reveal a dipole process that peaks beyond 100 kHz. At 2 and 3 h, the contributions from ϵ''_{ions} and the dipole process are displaced to lower frequencies; at 4 and 5 h, the broad loss feature appears to have structure. At later times, the loss curves are broad and become essentially independent of time (i.e., the dielectric properties become stationary, which is consistent with the chemical reaction going to completion and an elastomer being formed at long times). This contrasts with the behavior of the 0, 10, and 20% DBP systems in which a glass is formed at long times. The same behavior is observed for the 40% DBP system (Figure 17); the dipole relaxation process has structure at $t_r = 6$ h, and the system becomes stationary at long times, with ϵ'' increasing at high frequencies. $\Delta\epsilon_\beta$ is difficult to estimate from the data of Figures 16 and 17 because the loss peak occurs at high frequencies, but information regarding its relaxation strength can be obtained from the plots of ϵ' vs $\log(f/\text{Hz})$ for 40% DBP shown in Figure 18. ϵ' values tend to become stationary at long times, as in Figure 17. At 22 h, ϵ' is ~ 4.75 at 100 kHz. Because ϵ_∞ for all dipole relaxation processes lies in the range 2.0–2.5, the relaxation strength $\Delta\epsilon = 4.75 - \epsilon_\infty = 2.25 - 2.5$ remaining beyond 100 kHz is greater than that ($6.65 - 4.75 = 1.9$) for the lower-frequency process. This is reminiscent of polystyrene/plasticizer systems studied previously¹⁶ where the dipolar plasticizer molecules contributed to both α and β processes, as discussed below.

The behavior for these reactive systems containing DBP can be rationalized using knowledge from earlier DRS studies of polymer/plasticizer systems¹⁶ and DRS studies of thermosetting systems by Rolla and co-workers,¹⁷ Johari and co-workers,¹⁸ and Williams and co-workers.^{1,2} Hains and Williams¹⁶ studied the DRS behavior of polystyrene/plasticizer(P) systems where P was DBP, tritolyl phosphate, or dioctyl phthalate. Because polystyrene is essentially nonpolar, all dipole relaxations were due to the motions of the P molecules. Both α and β processes were observed for low P concentrations. The β process was due to *partial relaxation* of the mean-squared dipole moment $\langle\mu^2\rangle$ of the P molecules. The residual relaxation strength was relaxed by the α process at lower frequencies through the large-scale motions of the polymer chains. Above a minimum P concentration [60%(w/w) for polystyrene/DBP], the α and β processes merged to form the $\alpha\beta$ process, which relaxed all of $\langle\mu^2\rangle$ for the P molecules. Thus, α , β , and $\alpha\beta$ relaxations of known origins occurred for those polymer/plasticizer systems. For thermosetting systems, Rolla and co-workers¹⁷ and Johari and co-workers¹⁸ showed that the dielectric $\alpha\beta$ process at short times moved to lower frequencies and separated into β and α processes as the reaction proceeded. The α process moved rapidly to ultralow frequencies, indicating the formation of a glass, whereas the β process remained above 100 kHz. Our recent work for a thermosetting system^{1,2} extended these^{17,18} and earlier studies where the products were glasses (see ref 1 for a summary) to systems in which a *glass* was formed below T_F and an *elastomer* was formed above T_F . Consider again the results for the DGEBA/PACM/DBP systems. For 0, 10,

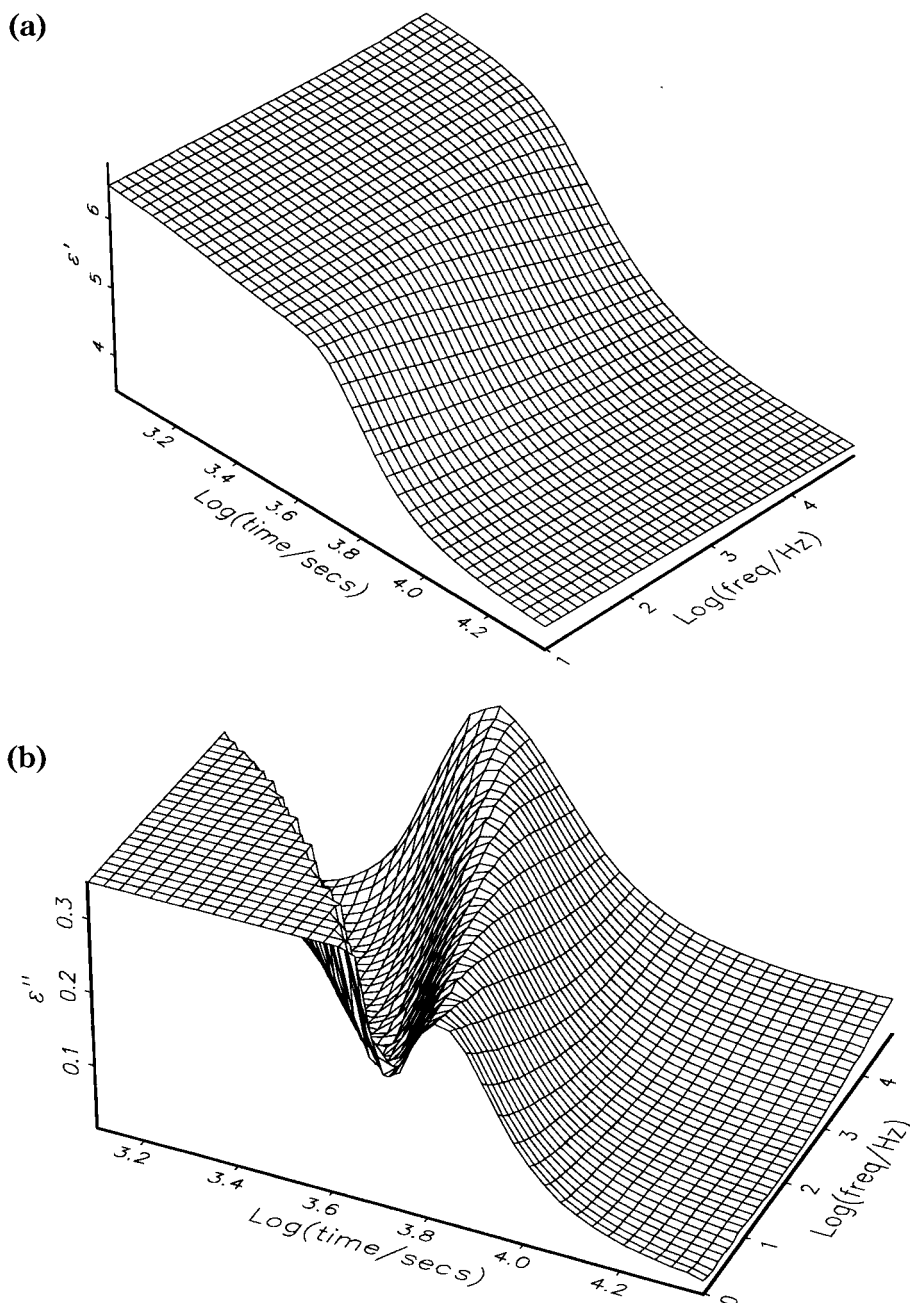


Figure 12. (a) ϵ' and (b) ϵ'' vs $\log(f/\text{Hz})$ and $\log(t_r/\text{s})$ for the 10% DBP system.

and 20% DBP, the dipole relaxation is an $\alpha\beta$ process at $t_r = 0$ and occurs at frequencies beyond our range. The $\alpha\beta$ process is due to the reorientational motions of monomeric species and DBP. As t_r increases, the $\alpha\beta$ process moves to lower frequencies and separates into β and α processes. $f_{\max}(\beta)$ is above 100 kHz at all times; $f_{\max}(\alpha)$ moves through the measurement range to ultralow frequencies. The product is a glass for each of these mixtures, so $T_R = 60^\circ\text{C} < T_F$. For the 30 and 40% DBP systems, similar behavior occurs at short times, with the β process peaking at high frequencies and the α process moving into the measurement range with time. However, the system becomes stationary when the α peak is in the kilohertz region, and an elastomer is formed at long times, so $T_R = 60^\circ\text{C} > T_F$ for these mixtures. In future studies, T_F values for the 10 and 20% DBP systems could be determined from DRS studies at $T_R > 60^\circ\text{C}$ until it is shown that an elastomer forms at long times. Similarly, T_F values for the 30 and

40% DBP systems could be obtained from DRS studies at $T_R < 60^\circ\text{C}$ until it is shown that a glass is formed at long times.^{1,2}

The DRS data for the DBP systems were converted to impedance data as described for the DGEBA/PACM/DEC systems. Figure 19 shows plots of $\log(-Z')$ vs $\log(f/\text{Hz})$ at different times for the 40% DBP system at 60°C . The behavior resembles that for the Decalin systems (e.g., Figure 5). Plots of $\log(f_{\max}(\sigma)/\text{Hz})$ vs $\log(t_r/\text{s})$ for 0, 10, 20, 30, and 40% DBP (Figure 20) show that $f_{\max}(\sigma)$ moves to very low frequencies with time. For the 0 and 10% DBP systems, the plots curve downward as $\log(f_{\max}(\sigma)/\text{Hz}) \rightarrow 0$, which suggests premonitory behavior for glass formation at long times, as for the 0, 10, and 20% Decalin systems. The curves for the 30 and 40% DBP systems at short times also suggest premonitory behavior for glass formation, but an inflection point is observed, and the slopes decrease at later times, indicating that the systems tend to become stationary at

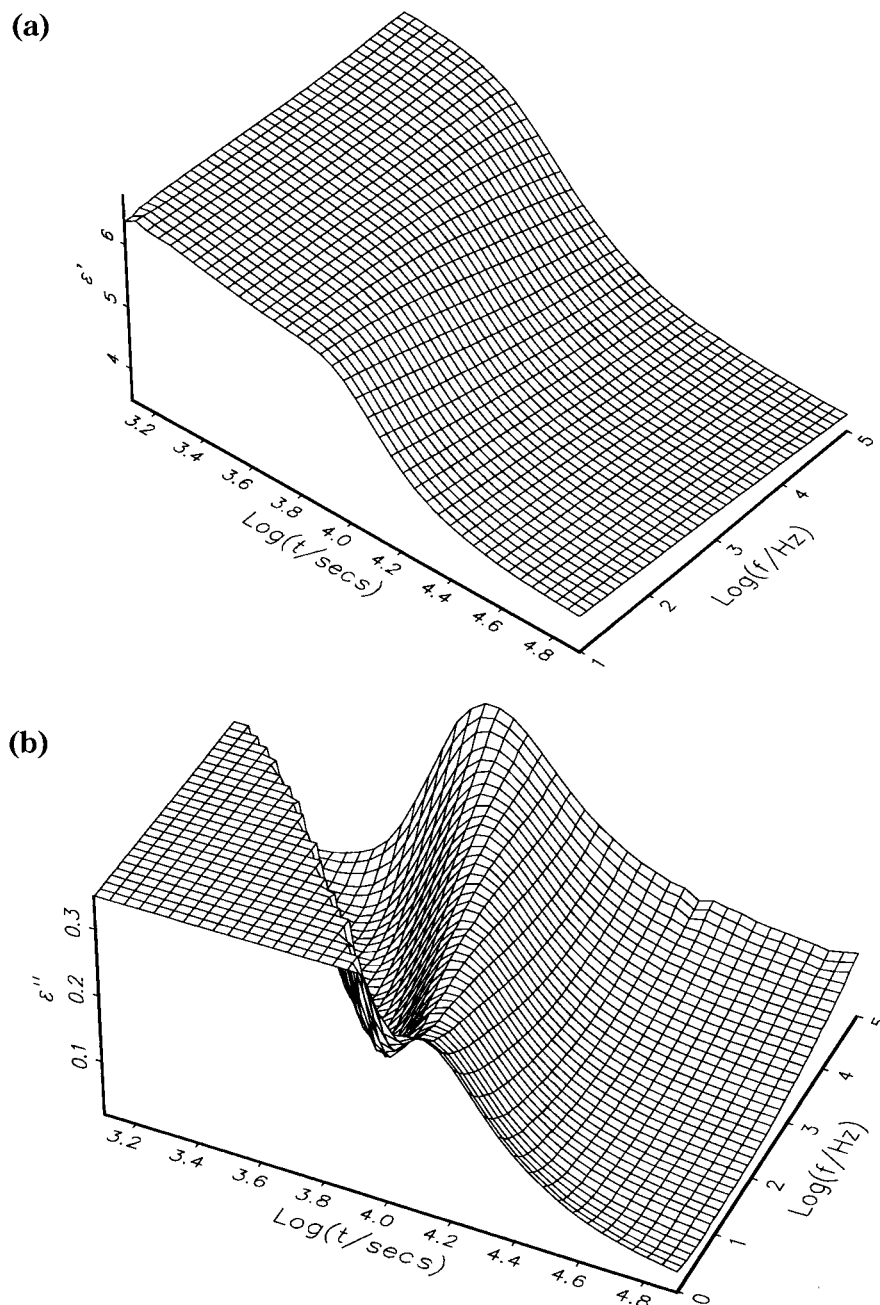


Figure 13. (a) ϵ' and (b) ϵ'' vs $\log(f/\text{Hz})$ and $\log(t/\text{s})$ for the 20% DBP system.

longer times. A comparison of the Z' and ϵ'' data demonstrates that molecular mobility (determined from the ϵ'' data) is still rapid when $f_{\text{max}}(\sigma)$ has fallen to 1 Hz, e.g., for the 30% DBP system $f_{\text{max}}(\sigma) = 1$ Hz at approximately 1.25 h (Figure 20). However, the ϵ'' data (Figure 16) show that the dipole relaxation processes are above 10^5 Hz at this time. Thus, changes in molecular mobility with time for these systems should be monitored using ϵ'' and not Z' data. The same conclusion applies to other thermosetting systems and is important when DRS is used as a practical method for cure-monitoring in industrial systems.

Width of Loss Curves and Fragility of the α Process

Consider again the form of plots of ϵ'' vs $\log t_r$ at constant f obtained in this study (e.g., Figure 1b). For

most dielectric relaxation functions, the frequency f and apparent relaxation time τ are complementary variables, as illustrated for the single relaxation time and the well-known KWW, Davidson–Cole, and Havriliak–Negami functions. Consider the plots of ϵ'' vs $\log(t/\text{s})$ at constant f and ϵ'' vs $\log(f/\text{Hz})$ at constant t_r . For those cases where a glass is formed at long times, both $\log(f)$ and $\log(f_{\text{max}})$ move to ultralow frequencies with time, and the loci of the points $[\log(f_{\text{max}}), \log(t_r)]$ and $[\log(f), \log(t_{r \text{ max}})]$ lie approximately on the same line.⁹ A plot of ϵ'' vs $\log t_r$ will show peaks at all frequencies down to 1 Hz and below if a glass is formed (e.g., for the 0% DBP system, Figure 8b). However, when an elastomer is formed, τ increases at first with time and then becomes constant at long times. Application of eq 1 shows that plots of ϵ'' vs $\log f$ at constant t_r will show peaks that becomes stationary with time when τ becomes independent of time. For this case, a plot of ϵ'' vs

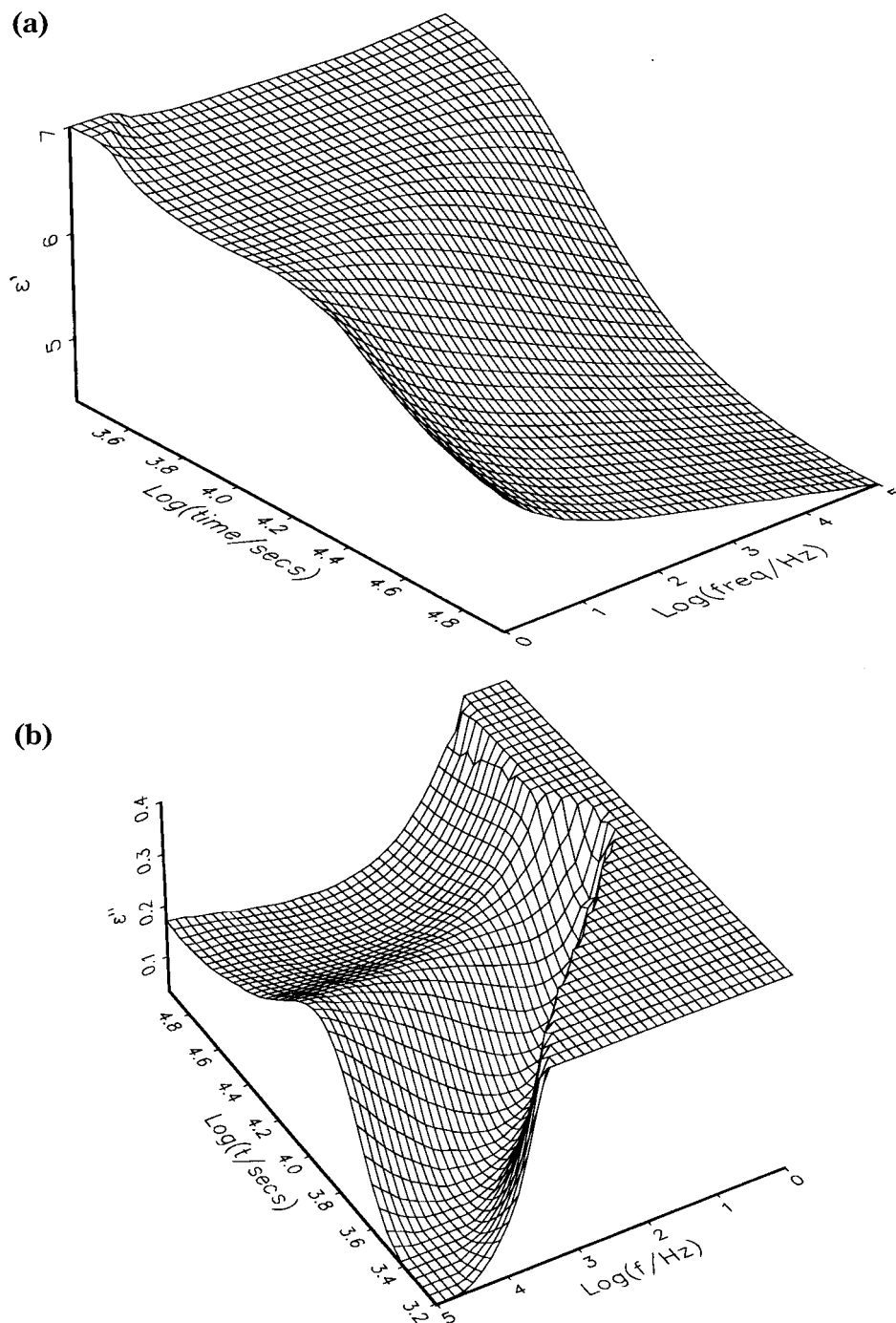


Figure 14. (a) ϵ' and (b) ϵ'' vs $\log(f/\text{Hz})$ and $\log(t/\text{s})$ for the 30% DBP system.

$\log(t_r)$ at constant frequency can show a peak if the frequency is sufficiently high, but the loss values will plateau at long times (e.g., Figure 8b for the 30% DBP system). At lower frequencies, ϵ'' can rise to a plateau and not show a peak (as we found for the epoxide/boroxine system; see Figure 8 of ref 1 for the system at 80 °C and $f = 10$ Hz).

The plot of ϵ'' vs $\log f$ at constant time for the Fuoss–Kirkwood function has a half-width $\Delta \log f = 1.144/n$. $\epsilon''_{\text{KWW}}(\omega)$ values obtained from the Fourier transform of the KWW function $\Phi_{\text{KWW}}(t) = \exp[-(t/\tau)^{\beta_{\text{KWW}}}]$ by Williams and co-workers^{19,20} and Koizumi and Kita²¹ give $\Delta \log f = [1.14/\beta_{\text{KWW}}]$ to good accuracy over the entire range of β_{KWW} . For a Fuoss–Kirkwood function,²² the half-width $\Delta \log t = \log(t_2/t_1)$ can be derived for a plot of ϵ'' vs $\log t_r$ at constant f , where t_2 and t_1 are the

values of t_r when $\epsilon'' = \epsilon''_{\text{max}}/2$. From eq 1, it follows that

$$\Delta \log \tau = \log[\tau(t_2)/\tau(t_1)] = \frac{1.144}{n} \quad (3)$$

Because $2\pi f\tau(t_m) = 1$ at the loss peak, the experimental relationship between $\log \tau$ and $\log t_r$ is determined from Figures 3 and 9. If one makes the approximation that these plots are linear in the range where ϵ'' goes from $\epsilon''_{\text{max}}/2$ at low f to $\epsilon''_{\text{max}}/2$ at high f (e.g., in Figures 1, 7, and 8) then $s = [-\Delta \log \tau / \Delta \log t]$ (from Figures 3 and 9). Hence, the half-width $\Delta \log t$ of the plot of ϵ'' vs $\log t_r$ is given by

$$\Delta \log t = \frac{1.144}{ns} \quad (4)$$

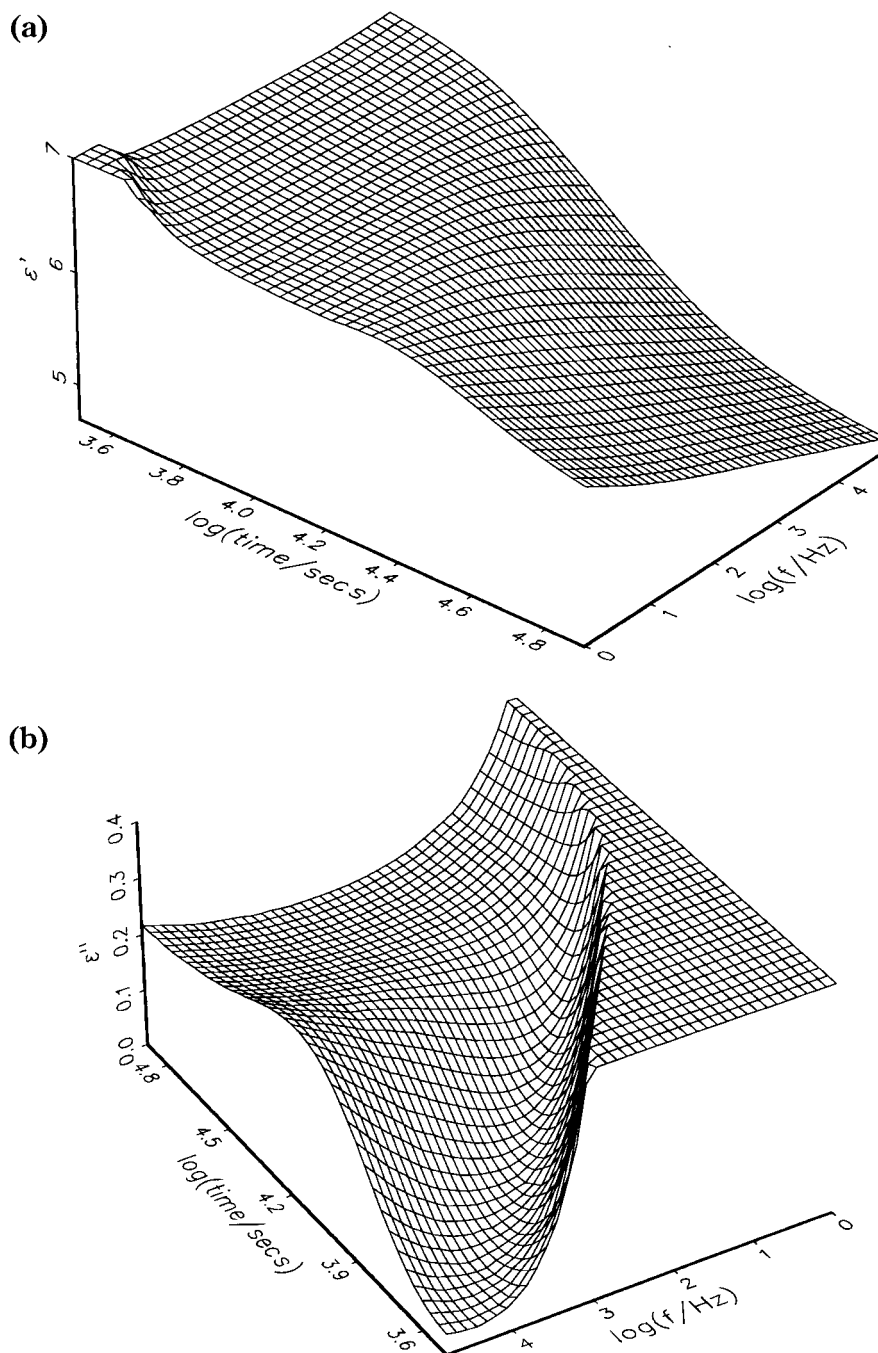


Figure 15. (a) ϵ' and (b) ϵ'' vs $\log(f/\text{Hz})$ and $\log(t/\text{s})$ for the 40% DBP system.

An examination of the plots of ϵ''_{KWW} vs $\log f$ obtained previously^{19–21} shows that the same result is obtained for the KWW function with n replaced by β_{KWW} . In the present study of DEGBA/PACM/diluent systems, the decrease in $|s|$ at constant frequency as c_{dil} increases (see Figures 3 and 9) leads to an increase in the half-width $\Delta \log t$, as seen in Figures 1, 7, and 8. Additionally, a broadening of the α -loss curves (decrease in m or β_{KWW}) during reaction will increase $\Delta \log t$, but it is difficult to determine changes in n or β_{KWW} from our data given the overlap of the α -loss peak with losses at low frequencies due to ions and at high frequencies due to the β process. For the epoxide/boroxine system studied previously,^{1,2} $\Delta \log t$ values (obtained from plots of ϵ'' vs $\log t_r$ at fixed frequencies for $T_R < T_F$) decrease with decreasing frequency (see Figure 12 of ref 2). In this case, $|s|$ increases with increasing $\log t_r$ in this f range

(see Figure 16b of ref 2), leading, from eq 3, to a decrease in $\Delta \log t$. Thus, the half-width of plots of ϵ'' vs $\log t_r$ for thermosetting systems can be understood, at least semiquantitatively, in terms of the breadth of the relaxation and $[\Delta \log \tau / \Delta \log t_r]$.

The influence of cross-linking on the shape and f location of the dielectric α process for amorphous polymers of different chemical structures has been studied previously.^{24–30} For cross-linked systems, the loss curves broaden (n or β_{KWW} decrease) and move to lower frequencies (T_g increases) as the degree of cross-linking is increased (see, in particular, ref 6 and the discussion above). In the present studies, and for many of the previous studies listed for thermosetting mixtures,^{1,2} the materials are (i) cross-linked and (ii) exhibit broad α relaxations, and (iii) T_g increases as the extent of cross-linking increases during reaction. Therefore,

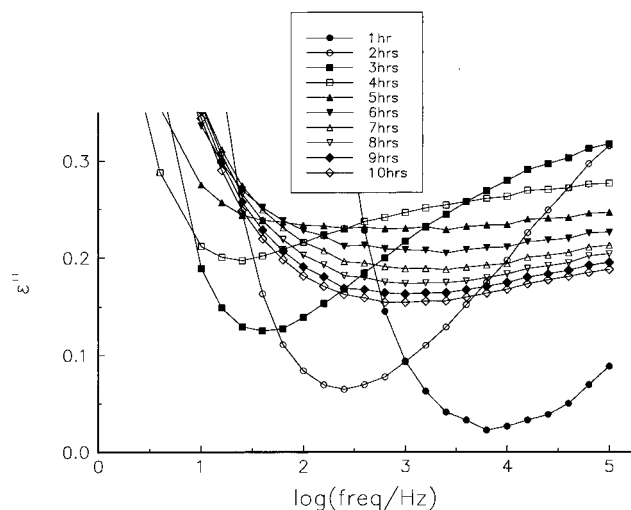


Figure 16. ϵ'' vs $\log(f/\text{Hz})$ for the 30% DBP system at different times.

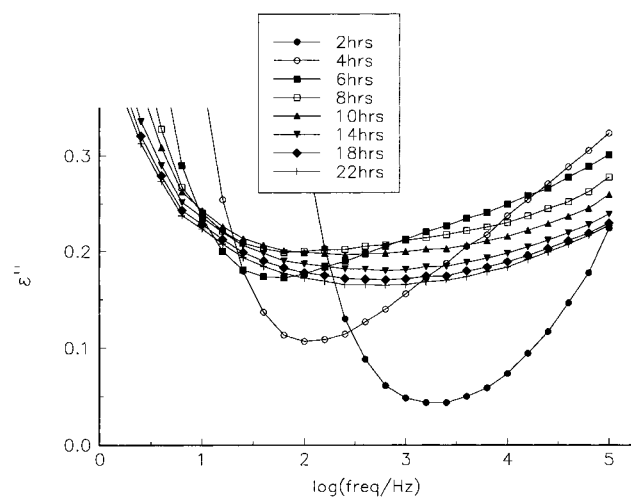


Figure 17. ϵ'' vs $\log(f/\text{Hz})$ for the 40% DBP system as for Figure 16.

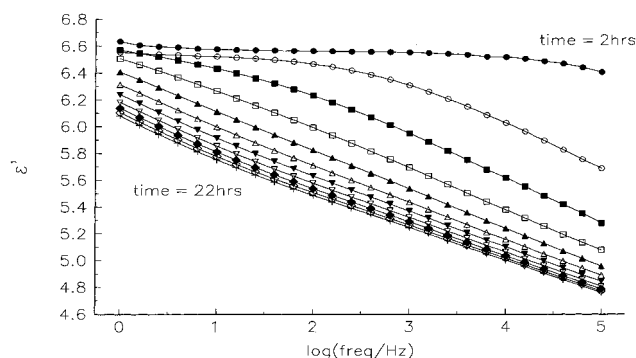


Figure 18. ϵ' vs $\log(f/\text{Hz})$ for the 40% DBP system recorded at 2-h intervals during reaction.

there are parallels between the DRS behaviors of reactive cross-linked systems and stationary cross-linked systems. There are also parallels between the dielectric α -relaxation behavior in these systems and those for glass-forming molecular liquids and amorphous polymers.³¹ At this point, a comment should be made concerning the cooperativity of the α process in different amorphous systems. The dielectric α relaxation is a fully cooperative process in *all* molecular glass-forming materials.³¹ For most glass-forming liquids and non-cross-linked amorphous polymers, the dielectric α

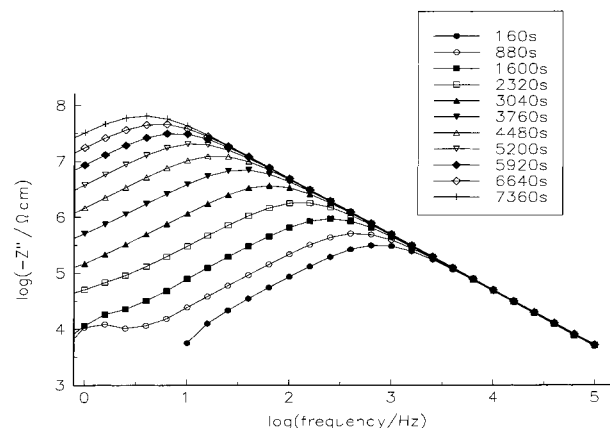


Figure 19. $\log(-Z')$ vs $\log(f/\text{Hz})$ for the 40% DBP system at different times.

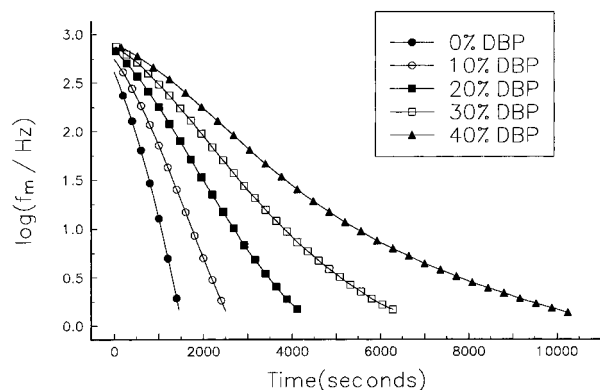


Figure 20. $\log(f_{\max}(t)/\text{Hz})$ vs time for 0, 10, 20, 30, and 40% DBP systems at different times.

process appears as an unstructured loss peak that can be fitted approximately using the KWW function and that has $\Delta \log f$ values at T_g in the range 1.6–2.3 (i.e., $\beta_{\text{KWW}} = 0.5$ –0.7). The dielectric α -loss peaks for materials of medium to high cross-link density^{6,24–30} are, at T_g , (i) broader than those in non-cross-linked materials and (ii) more symmetrical than those calculated for the KWW function.^{19,20} Result i suggests that these materials are heterogeneous microscopically (see ref 2 for a discussion), and result ii arises because the restricted motions of chains near the cross-links^{1,6,25} make their main contribution to the loss peak at frequencies *below* f_{\max} .

Recently, Yu Kamarenko and co-workers³⁰ reported extensive DRS studies of the α process in model heterocyclic polymer networks. They found that both T_g and $\Delta \log f$ increased as the cross-link density was increased. As part of their analysis of the changes in the relaxation maps as cross-link density increased, they used the concept of fragility introduced by Angell.^{14,32–35} He and other workers^{36–38} applied the Vogel–Fulcher–Tammann equation for $\langle \tau_\alpha(T) \rangle$ to data for different glass-forming liquids and amorphous polymers obtained from different relaxation and scattering techniques and developed the concept of the fragility of the process. We now consider whether this approach can be applied to the reactive systems studied here and previously.^{1,2,4}

The Vogel–Fulcher–Tammann (VFT) equation for the dependence of $\langle \tau(T) \rangle$ on temperature (T) is given by

$$\langle \tau(T) \rangle = A \exp[B/(T - T_0)] \quad (5)$$

where A , B , and T_0 are material constants. Angell

rescaled ($1/T$) as (T_g/T) ($=x$ say) and plotted $\log \langle \tau \rangle$ vs (T_g/T). A fragility index m can be defined^{32,38} as the slope ($d \log \tau / d(T_g/T)$) at $T = T_g$. In a recent DRS study of a low-molar-mass glass-forming liquid, chiral isooctyloxy-cyanobiphenyl,³⁹ eq 4 was rearranged to a rescaled form and, omitting $\langle \tau \rangle$ for brevity, gave

$$\frac{\log \tau(T) - \log \tau(T_g)}{\log \tau_\infty - \log \tau(T_g)} = \frac{[1 - x(T)](1 - \alpha)}{1 - \alpha x(T)} \quad (6)$$

Alternatively

$$\frac{\log \tau(T) - \log \tau_\infty}{\log \tau(T_g) - \log \tau_\infty} = \frac{x(T)(1 - \alpha)}{1 - \alpha x(T)} \quad (7)$$

where $\tau_\infty = \tau(T \rightarrow \infty)$ and $\alpha = T_0/T_g$. Also $T_g = T_0 + B/\Delta$, where $\Delta = [\log \tau(T_g) - \log \tau_\infty]$. In the rescaled forms, $\log \tau(T)$ is a function of x and α . In the works of Angell,^{32–34} $\log \tau(T_g) = 2$, and $\log \tau_\infty = -14$, so $\Delta = 16 T_0$. The fragility index^{32,38} $m = \Delta/(1 - \alpha)$. Because Δ is fixed, m depends solely on α .

For the cross-linked materials studied by Yu Kamarenko and co-workers,³⁰ their Table 3 shows that (i) T_g increases from 287.6 to 362.0 K, (ii) T_0 increases from 193 to 276.8 K, (iii) $(T_g - T_0)$ is approximately constant at 84 ± 3 K, and (iv) α increases from 0.67 to 0.76 as the initial molar ratio (L/N) varies from 100/0 to 0/100, i.e., as the cross-link density increases. Thus, the fragility index increases with increasing cross-linking density in these model systems. In the case of polymerizing systems of the kind studied here, both T_g and T_0 increase during reaction, as we have discussed.² If $(T_g - T_0)$ is approximately constant during reaction, then as T_g increases $\alpha = (T_0/T_g) \rightarrow 1$, so the fragility index increases correspondingly. We are led to the following conclusions for cross-linked thermosetting systems: (a) As the reaction proceeds the α relaxation moves to ultralow frequencies (e.g., as in Figure 9), so T_g and T_0 of the system at each time increase, leading to an increase in α and hence an increase in the fragility index for the process with time (see ref 2 for a discussion of how an increase in T_g during reaction is related to the TTT diagram of Gillham). (b) Because T_g and T_0 decrease as c_{dil} increases, then from a comparison of the DRS data for undiluted and diluted systems at a fixed time during reaction (see Figure 9), it appears that the fragility index of the diluted system is less than that of the undiluted system at that time. In the recent work of Andjelic and Mijovic,⁶ discussed above for the 50/50 formulation, it appears from their Figure 16 that there is an overall increase in the fragility index as the degree of conversion increases from 0 to 80%.

Acknowledgment. The authors thank the EPSRC for a Case Award to I.K.S. and for a grant for the purchase of the Novocontrol Dielectric Spectrometer. G.W. thanks the Leverhulme Trust for an Emeritus Fellowship.

References and Notes

- (1) Williams, G.; Smith, I. K.; Holmes, P. A.; Varma, S. *J. Phys. Condens. Matter* **1999**, *11*, A57-A74.
- (2) Williams, G.; Smith, I. K.; Aldridge, G. A.; Holmes, P. A.; Varma S. *Polymer* **2001**, *42*, 3533.
- (3) (a) Gillham, J. K. *Polym. Eng. Sci.* **1986**, *26*, 1430. (b) Gillham, J. K.; Chan, L. C.; Kinloch, A. J.; Shaw, S. J. In *Abstracts of the Plastics and Rubber Institute International Conference on the Toughening of Plastics, July 1985*; Plastics and Rubber Institute: London, U.K., 1985.
- (4) Fournier, J.; Williams, G.; Duch, C.; Aldridge, G. A. *Macromolecules* **1996**, *29*, 7097.
- (5) Partridge, I. K.; Maistros, G. M. *High Perform. Polym.* **1996**, *8*, 1.
- (6) Andjelic, S.; Mijovic, J. *Macromolecules* **1998**, *31*, 2872.
- (7) Smith, I. K.; Andrews, S. R.; Williams, G.; Holmes, P. A. *J. Mater. Chem.* **1997**, *7*, 203.
- (8) McCrum, N. G.; Read, B. E.; Williams, G. *Anelastic and Dielectric Effects in Polymeric Solids*; Dover: New York, 1991.
- (9) Smith, I. K. Ph.D. Thesis, University of Wales, Swansea, U.K., 1997.
- (10) Mijovic, J.; Yee, C. F. W. *Macromolecules* **1994**, *27*, 7287.
- (11) Mijovic, J.; Bellucci, F.; Nicolais, L. *J. Electrochem. Soc.* **1995**, *142*, 1176.
- (12) Bellucci, F.; Valentino, M.; Monetta, L.; Nicodemo, L.; Kenny, J.; Nicolais, L.; Mijovic, J. *J. Polym. Sci. B: Polym. Phys.* **1995**, *32*, 2519.
- (13) Bellucci, F.; Valentino, M.; Monetta, L.; Nicodemo, L.; Kenny, J.; Nicolais, L.; Mijovic, J. *J. Polym. Sci. B: Polym. Phys.* **1995**, *33*, 433.
- (14) Angell, C. A. *J. Non-Cryst. Solids* **1991**, *131–133*, 13.
- (15) Ngai, K. L.; Plazek, D. J. *Rubber Chem. Technol.* **1996**, *68*, 376.
- (16) Hains, P. J.; Williams, G. *Polymer* **1975**, *16*, 725.
- (17) Casalini, R.; Corezzi, S.; Fioretto, D.; Livi, A.; Rolla, P. A. *Chem. Phys. Lett.* **1996**, *258*, 470.
- (18) Cassettari, M.; Salvetti, G.; Tombari, E.; Veronesi, S.; Johari, G. P. *J. Non-Cryst. Solids* **1994**, *172–174*, 554.
- (19) Williams, G.; Watts, D. C. *Trans. Faraday Soc.* **1970**, *66*, 80.
- (20) Williams, G.; Watts, D. C.; Dev, S. B.; North, A. M. *Trans. Faraday Soc.* **1971**, *67*, 1323.
- (21) Koizumi, N.; Kita, Y. *Bull. Inst. Chem. Res., Kyoto Univ.* **1978**, *56*, 300.
- (22) This analysis resembles that for $\Delta \log f$ of plots of ϵ'' vs T^{-1} at fixed f by Read and Williams.^{8,23}
- (23) Read, B. E.; Williams, G. *Trans. Faraday Soc.* **1961**, *57*, 1979.
- (24) Schlosser, E.; Schonhals, A. *Colloid Polym. Sci.* **1989**, *267*, 133.
- (25) Glatz-Reichenbach, J. K. W.; Sorriero, L. J.; Fitzgerald, J. J. *Macromolecules* **1994**, *27*, 1338.
- (26) Casalini, R.; Fioretto, D.; Livi, Lucchesi; Rolla, P. A. *Phys. Rev. B* **1997**, *56*, 3016.
- (27) Kannurpatti, A. R.; Bowman, Ch. N. *Macromolecules* **1998**, *31*, 3311.
- (28) Nicolai, T.; Prochazka, F.; Durand, D. *Phys. Rev. Lett.* **1999**, *82*, 863.
- (29) Fitz, B.; Mijovic, J. *Macromolecules* **1999**, *32*, 3518.
- (30) Yu Kamarenko, V.; Ezquerro, T. A.; Sics, I.; Balta-Calleja, F. J. *J. Chem. Phys.* **2000**, *113*, 447.
- (31) Williams, G. In *Dielectric and Related Molecular Relaxation Processes*; Davies, M. M., Ed.; Specialist Periodical Reports; The Chemical Society: London, 1975; p 151–182.
- (32) Angell, C. A. In *Relaxations in Complex Systems*; Ngai, K. L., Wright, G. B., Eds.; National Technology Information Service, U.S. Department of Commerce: Springfield, VA, 1985; p 1.
- (33) Angell, C. A. *J. Non-Cryst. Solids* **1991**, *131–133*, 13.
- (34) Angell, C. A. *Polymer* **1997**, *38*, 6261.
- (35) Böhmer, R.; Ngai, K. L.; Angell, C. A.; Plazek, D. J. *J. Chem. Phys.* **1993**, *99*, 4201.
- (36) Plazek, D. J.; Ngai, K. L. *Macromolecules* **1991**, *24*, 1222.
- (37) Böhmer, R.; Angell, C. A. *Phys. Rev. B* **1992**, *45*, 10091.
- (38) Böhmer, R. *J. Non-Cryst. Solids* **1994**, *172–174*, 628.
- (39) Massalska-Arodz, M.; Williams, G.; Thomas, D. K.; Jones, W. J.; Dabrowski, R. *J. Phys. Chem. B* **1999**, *103*, 4197.

MA010335G